3D VISUALIZATION FOR EARTHQUAKE-INDUCED SITE LIQUEFACTION POTENTIAL BASED ON VOLUME RENDERING AND GIS TECHNOLOGY

Hao Tang[1] and Guo-xing Chen[2]

[1] *PH. D, Dept. of Civil Engineering, Institute of Geotechnical Engineering, Nanjing, China*
[2] *Professor, Dept. of Civil Engineering, Institute of Geotechnical Engineering, Nanjing, China*
Email: th_njut@126.com

ABSTRACT :

The research on visual 3D modeling for the earthquake-induced site liquefaction potential is to resolve the problem of simulating the potential risk of earthquake-induced site liquefaction spatially by 3D reality graphics. And it can be applied to the urban earthquake prevention and disaster mitigation. Firstly, the empirical equation of cyclic resistance ratio *CRR* of saturated sands with different probability levels is utilized to evaluate the earthquake-induced site liquefaction potential. Secondly, a “block” data structure is adopted to describe the 3D liquefaction potential entity. Thirdly, visual 3D visualization modeling for the earthquake-induced site liquefaction potential can be realized based on the Kriging interpolation method and volume rendering technique. The research described in this paper shows that: (1) When 3D liquefaction potential entity is partitioned by the “block” data model, the Kriging method can be adopted to realize 3D interpolation. Therefore, the latent distribution of the site liquefaction potential beyond the observation boreholes can be evaluated. (2) Based on the probability evaluation results and volume rendering technique, the Kriging interpolation results are displayed in different color marks to indicate the risk extent of the site liquefaction potential. Thereby, the spatial distributing characteristics and variety trend of the site liquefaction potential can be displayed in the 3D graphic form. And also, the 2D profile cutting and 3D body incision can be generated automatically.

KEYWORDS: earthquake-induced liquefaction potential, sand liquefaction probabilistic estimation method, 3D Modeling, Kriging interpolation method, volume rendering, GIS

1. INTRODUCTION

The risk evaluation for earthquake-induced site liquefaction potential is vital to the region planningt, route determination, building location selection and earthquake-induced geologic disasters prevention etc. As the influence factors on the site liquefaction and the liquefaction disaster itself present the spatial distribution characteristics. So it is important to construct the corresponding 3D model according to the scattered borehole data, and display the risk evaluation results of earthquake-induced site liquefaction potential in 3D graphics. And it will be helpful to the earthquake engineering researchers to understand the spatial distributing regularity of the earthquake-induced site liquefaction potential.

Literatures about GIS applied in the earthquake-induced site liquefaction potential evaluation have shown the potential of GIS technology, but most of them emphasize on the test results from deterministic methods, such as SPT (standard penetration test), CPT (cone penetration test) and Vs (shear wave velocity) etc. In these applications, GIS is just adopted as a data preparation and management tool for visual 2D evaluation and not for 3D analysis modeling of earthquake-induced site liquefaction potential. However, for important engineering projects, the earthquake-induced geologic disaster must be considered in the design stage and the distributing of site liquefaction potential presents the typical 3D characteristic. Therefore, it is necessary to construct a visual 3D visualization model for the earthquake-induced site liquefaction potential based on the GIS technology.

Based on GIS and probability evaluation model of the site liquefaction potential, a 3D visualization model is put forward by coupling 3D interpolation method and volume rendering technique. Therefore, the probability evaluation results can be displayed in 3D graphics, and the contents discussed in this paper may provide some instructive advices in 3D modeling for the earthquake-induced site liquefaction potential.

2. IDEAL AND KEY METHODS

2.1. Research Ideal

Limited to the external conditions, the sampling data can not be acquired adequately to realize the 3D visualization model. Thereby, more sampling points must be generated based on spatial interpolation of these original points. When the scattered interpolation points are generated, the engineering site can be partitioned by a series of cube units. The attribute in every unit is homogeneous, and this attribute represents the evaluation result of liquefaction potential at this site point. Therefore, the variation regularity of attribute in these units becomes the distributing characteristics of the site liquefaction potential. Based on 3D volume rendering technique, the interpolation results are displayed in different color marks, and the 3D graphics of the site liquefaction potential can be generated. Also, 2D profile cutting and 3D body incision can be realized automatically.

The ideal in this paper is as the follows:

(1) Format transformation of interpolation data. Based on the DEM (Digital Elevation Model) ideal, the evaluation value of the site liquefaction potential is adopted as "Elevation" and 3D information in GIS is transformed into the data format that is supported by a visuallization software, 3D Surfer.

(2) 3D interpolation of scattered data. At present, most GIS software can only realize 2D plane interpolation. Therefore, 3D surfer is adopted to realize 3D interpolation in this paper. One attribute value named as *I*, which represents the evaluation result of site liquefaction potential, is added into the scattered data. Therefore, 3D data field of the site liquefaction potential is expressed as $u=f(X, Y, Z, I)$.

(3) Classification and assignment of interpolation results. When the 3D data field is generated by spatial interpolation, based on volume rendering technique, the partition unit can be displayed in different color marks or diaphaneity. Thereby, 3D model for site liquefaction potential is generated.

(4) 3D analysis of the site liquefaction potential. Based on 3D volume imaging, 2D profile cutting and 3D body incision are realized automatically. Therefore, the 3D functions, which can not be achieved by 2D and 2.5D GIS analysis, can be realized.

Therefore, the modeling process for 3D visualization in the earthquake-induced site liquefaction potential is shown as Figure.1.

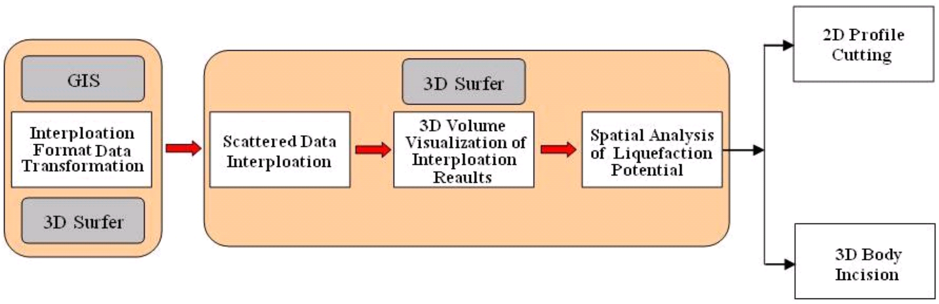

Figure 1 The modeling process for 3D visualization in earthquake-induced site liquefaction potential

2.2. Probability Evaluation Model of Earthquake-induced Site Liquefaction Potential

Based on 344 liquefaction site data in 25 strong earthquakes, the limit state function CRR_{cri} (Critical Cyclic Resistance Ratio) is constructed to estimate the sandy soil liquefaction based on the RBF (radial basis function) neural network method (G. X. Chen et al., 2006). Therefore, the critical cyclic resistance ratio CRR_{cri} can be calculated by the following formula:

$$CRR_{cri} = 0.0002N_1^2 + 0.005N_1 + 0.03 \quad (1)$$

Where, N_1 is the SPT blow count normalized to an overburden pressure of approximately 100 kPa (1 ton/sq ft) and a hammer energy ratio or hammer efficiency of 60%.

When the equivalent cyclic stress ratio *CSR* of a sandy soil layer caused by the earthquake ground motion is greater than CRR_{cri} determined in formula (1), the saturated sandy soil layer will be a liquefaction case, otherwise a non-liquefied case.

Thus, the probability function to estimate the sandy soil liquefaction can also be set up according to the relationship $F_s = CRR_{cri}/CSR$, F_s is the cyclic resistance safety factor and P_L is liquefaction probability.

$$P_L = 1/(1+F_s^{\ 4.297}) \tag{2}$$

Combine formula (1) and (2), the sandy soil liquefaction resistance stress curve under the different probability can be shown as the follows:

$$CRR = [P_L/(1-P_L)]^{0.233} \cdot CRR_{cri} \tag{3}$$

Table 1 Standard for probability evaluation

Liquefaction probability level P_L	Sand liquefaction safety factor F_s	Liquefaction potential evaluation
$0.00 \leqq P_L < 0.30$	$F_s \geqq 1.2$	non-liquefaction
$0.30 \leqq P_L < 0.70$	$0.81 < F_s < 1.2$	possible liquefaction
$0.70 \leqq P_L < 1.00$	$F_s \leqq 0.81$	liquefaction

As the Table 1 shows, three grades are classified to identify the liquefaction potential of saturated sandy soil according to the different liquefaction probability level. Therefore, the probabilistic estimation of earthquake-induced site liquefaction can be done as the follows: Firstly, one acceptable liquefaction probability level must be confirmed according to the importance of the engineering project. Secondly, the estimation criteria of sandy soil liquefaction (*CRR*) with different probability can be calculated by formula (3). Thus, the calculated *CRR* can be compared with the *CSR*.

2.3. Evaluation of Earthquake-induced Site Liquefaction Potential Based on 3D Interpolation and Volume Rendering

At present, it is still difficult to construct 3D model for the earthquake-induced site liquefaction potential based on GIS. Therefore, one "block" data structure] is introduced in the research, and the *SEE* (Spatial Entity Enumeration) method is adopted to describe 3D entity. Also, the 3D modeling research is realized by coupling 3D interpolation and volume rendering technique.

2.3.1 "Block" Data Model Applied in 3D Modeling

In the 3D GRID model, the objective space is partitioned by a mount of regular 3D grid, so the space is expressed as the grid assembly. In fact, the 3D GRID model can be seen as the extension of a 2D GRID model in 3D space. Therefore, 3D GRID model is adopted to construct 3D data field in the research, and one "block" model is introduced to realize the visual 3D visualization model for the earthquake-induced site liquefaction potential.

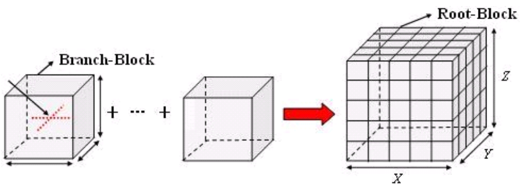

Figure 2 Block model definition

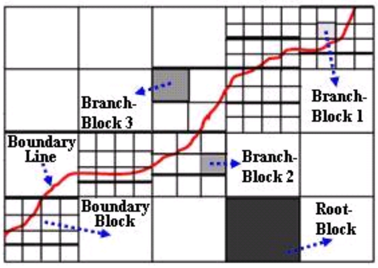

Figure 3. Relation between block and sub-block in boundary simulation

The "block" mode is an effective data mode to partition the site and to simulate the site's interior characters. It divides the site into a series of small cubes. The cube size is determined by whether every cube has a uniform interior attribute, and the attribute must represent interior attribute at the exact site point. The model, accumulating such cubes to simulate the site's interior characters, is named as "block" mode. The cube, which has one attribute, is named as element block. The element block is classified into "root-block" or "branch-block", and the "root-block" is the biggest cube allowed in the model, the "branch-block" is the smaller cubes, which is part of the partitioned "root-block". The "root-block"' size is determined by the borehole distance, geologic condition and the research precision. The "root-block" partition is shown in Figure.2. Figure.3 shows the relation map between "root-block" and "branch-block" in site characters simulation. Seen from Figure.3, the little the "branch-block" size is, the more accurate the boundary line simulation will be.

As the GRID model, "block" model can be easily realized in a computer easily, and the reliable interpolation results can be obtained. Also, it calculates so rapidly and the simulatipn of the boundary line of the 3D liquefaction potential field can be obtained accurately.

2.3.2 Kriging Method Applied in the Interpolation of Liquefaction Potential

Based on Kriging interpolation method, the variogram function is utilized to simulate the spatial characteristics of earthquake-induced site liquefaction potential. Therefore, the liquefaction potential of unidentified site points can be evaluated by the original observation boreholes.

(1) Basic interpolation principle

Soil property presents to be special variant. However, there is still certain relativity between the different soil points, viz. the vertical or horizontal relativity and variability. Therefore, the attributes of the site soil liquefaction potential can be generally expressed by regional variable $z(x)$.

$z(x_i)(i=1,2,\cdots n)$ is assumed as a set of scattered liquefaction potential value of sampling points, and these values are second-order stationary. In order to estimate the true liquefaction potential value at arbitrary point x_0 in the identified region, the best appraisal value $z^*(x_0)$ is assumed as the linear combination of $z(x_i)$:

$$z^*(x_0)=\sum_{i=1}^{n}\lambda_i z(x_i) \tag{4}$$

Where, λ_i is the weight coefficient; $z^*(x_0)$ is the appraisal value at the position x_0; i is the serial number of the borehole.

(2) Kriging Interpolation Equations

The principle of Kriging interpolation is to make sure this appraisal value $z^*(x_0)$ is unbiased estimator, and the estimated variance is less than the value of any other linear combination. Therefore, Kriging interpolation equations can be shown as the follows:

$$\begin{cases}\sum_{i=1}^{n}\lambda_i\gamma(x_i,x_j)+\mu=\gamma(x_j,x_0) \quad (i,j=1,2,\cdots,n)\\ \sum_{i=1}^{n}\lambda_i=1\end{cases} \quad \text{Viz.} \quad \begin{vmatrix}\gamma_{11} & \cdots & \gamma_{1n} & 1\\ \cdots & \cdots & \cdots & \cdots\\ \gamma_{n1} & \cdots & \gamma_{nn} & 1\\ 1 & \cdots & 1 & 0\end{vmatrix}\begin{vmatrix}\lambda_1\\ \cdots\\ \lambda_n\\ \mu\end{vmatrix}=\begin{vmatrix}\gamma_{01}\\ \cdots\\ \gamma_{0n}\\ 1\end{vmatrix} \tag{5}$$

Where, $\gamma_{ij}=\gamma(x_i,x_j)$ is the variogram function value between x_i and x_j; μ is the Lagrange multiplier. When the weight coefficient λ_i and Lagrange multiplier μ are obtained after resolving the Kriging equations (5), the best appraisal value $z^*(x_0)$ can also be estimated according to the formula (4).

2.3.3 Introduction of 3D Vplume Rendering

The volume rendering technique involves the expression, analysis, operation and display etc. of 3D volume data and its primary aim is to discover the complex inner structure of an object. The primary difference between volume rendering and computer graphics technique is as the follows:

(1) The volume rendering technique is the collection of limited and scattered sampling data, but the computer graphics technique is the continuous geometry description. Therefore, the management, operation, transformation, analysis and display methods of objects are also different entirely.

(2) Surface and side boundary primitives (basic dollar) are utilized to describe the object in traditional computer graphics, and it does not t contain any inner information. However, in the volume rendering technique, the 3D primitive is adopted to describe the object and the whole object information inside and

outside is expressed distinctly.

Though the volume data structure is different from each other, and their distributions and relations are also different. The basic process of the volume rendering technique is the same generally. Figure 4 shows the process of volume rendering applied in 3D modeling of the earthquake-induced site liquefaction.

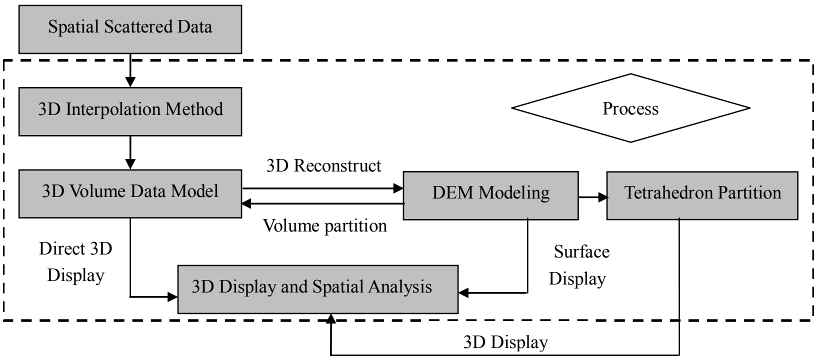

Figure 4 The process of volume rendering applied in 3D modeling of site liquefaction potential

3 EXAMPLE ANALYSIS

One actual engineering example is adopted to illustrate the 3D visualization modeling for the earthquake-induced site liquefaction potential based on the spatial interpolation method and volume rendering. Figure 5 shows the spatial distribution of the reconnaissance boreholes in a engineering site. In this paper, twenty-two avail boreholes including 118 SPT points are adopted to estimate the earthquake-induced site liquefaction potential based on the probability evaluation model mentioned above. Table 2 shows the soil parameters and the probabilistic estimation result of the identified borehole soil, and i is the serial number of borehole, X and Y are the plane coordinates (unit: meter), Z is the SPT midpoint depth (unit: meter), and P_L is the probability evaluation result.

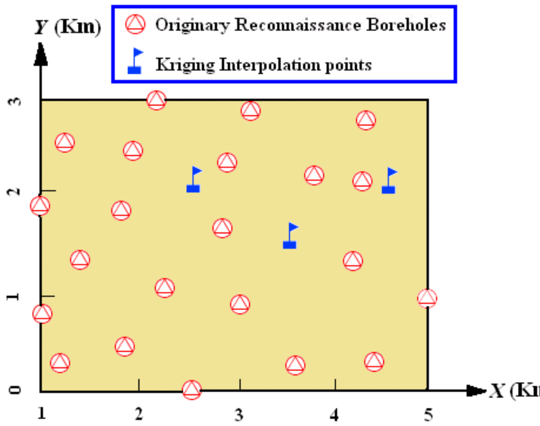

Figure 5 The distributing map of original bore liquefaction potential

118 scattered points with spatial coordinates are acted as the spatial interpolation points to generate the 3D grid data file. Therefore, the whole engineering site is expressed in a series of small cubes, and the cube color represents the liquefaction potential extent at this point. In this paper, 100×100×100=1000000 rectangles are defined in x, y, z axis.

Figure 6 is a 3D display of the original 118 scattered points, and the deeper the color is, higher the liquefaction potential risk will be. Figure 7 shows the 3D digital model of site liquefaction potential after 3D interpolation and data girded. Thereby, the advanced spatial analysis can be done based on this 3D model.

Figure 8, 9 and 10 are the 3D stratified display of the earthquake-induced site liquefaction potential, including non-liquefaction, possible liquefaction and liquefaction stratum. When the stratum with different liquefaction potential risk is displayed independently, it will be helpful to the prevention and mitigation of earthquake-induced city disasters.

Based on the 3D model as shown in Figure 7, the 3D body incision and 2D profile of the liquefaction potential can be realized easily. In 3D Surfer, the body incision is completed in rectangle format, and the incision body is defined by the coordinate size in x, y, z axis. When the incision is done, it will calculate again to display the 3D map, which will only show the 3D model after the incision. The 2D cutting profile is classified into three types, which are vertical to x, y, z axis respectively.

Table 2 Probabilistic analysis results of site soil liquefaction potential

i	X	Y	Z	P_L
1	4144.41	1287.41	2.25	0.040
			10.50	0.044
2	1233.83	345.49	1.95	0.398
			5.65	0.101
			10.90	0.127
3	1024.31	833.15	3.15	0.378
			5.15	0.409
			11.05	0.077
4	4207.30	2104.67	5.90	0.815
			8.15	0.904
			8.90	0.935
			10.50	0.856
			11.90	0.913
			13.70	0.616
			14.40	0.636
5	4338.53	298.15	4.90	0.864
			6.00	0.921
			7.00	0.934
			8.00	0.853
			9.00	0.918
			10.60	0.965
			11.70	0.893
			12.70	0.933
			13.90	0.263
			14.60	0.159
6	1948.79	2509.05	6.55	0.924
			9.20	0.985
			11.25	0.926
			13.70	0.884
			15.50	0.646
			18.50	0.213
7	2839.49	1759.37	10.50	0.600
8	3852.94	2168.72	10.80	0.930
9	1187.31	2634.11	10.50	0.402
10	2843.54	2246.74	1.75	0.947
			2.75	0.863
			3.75	0.849
			4.75	0.901
			8.75	0.470
			9.75	0.029
			13.15	0.062
			14.65	0.117
			16.15	0.046
			17.65	0.008
			19.65	0.199
11	3098.41	2957.21	5.65	0.552
			7.05	0.993
			7.75	0.606
			9.75	0.990
12	2653.56	106.54	2.10	0.435
			3.10	0.502
			8.10	0.159
			9.10	0.199
			10.10	0.709
			12.10	0.124
			13.10	0.447
13	1432.50	1316.57	2.80	0.358
			4.90	0.770
			7.00	0.057
14	4297.21	2736.24	5.70	0.008
			6.65	0.968
			8.80	0.976
			10.20	0.982
			11.75	0.991
			13.10	0.991
			14.70	0.979
			16.20	0.956
			17.75	0.240
			19.15	0.048
			7.05	0.993
			7.75	0.606
			9.75	0.990
15	1923.71	498.77	4.80	0.340
			5.80	0.784
			6.80	0.894
			7.80	0.948
			8.80	0.823
			11.10	0.292
			12.30	0.506
16	1008.93	1882.98	5.40	0.895
			7.40	0.914
			9.30	0.947
			14.30	0.953
			18.90	0.729
17	2312.75	1027.41	4.90	0.133
			5.90	0.474
			6.90	0.559
			7.90	0.422
			8.90	0.484
			9.90	0.775
			10.90	0.739
			11.90	0.700
			12.90	0.888
18	4966.67	916.53	3.20	0.563
			4.20	0.945
			6.60	0.845
			7.70	0.151
19	2831.43	1756.20	4.20	0.264
			5.35	0.847
			6.35	0.932
			6.80	0.832
			7.70	0.912
			8.80	0.926
			10.40	0.891
			11.80	0.984
20	2192.27	2886.84	5.35	0.912
			5.80	0.958
			6.80	0.896
			7.80	0.949
			8.80	0.926
			10.90	0.499
			11.90	0.221
21	1986.63	2492.38	6.50	0.978
			8.40	0.465
			10.80	0.147
22	3655.52	243.15	6.60	0.968
			10.60	0.991
			20.00	0.292

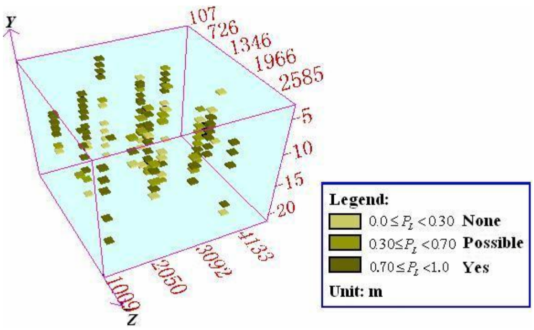

Figure 6 3D display of scattered data

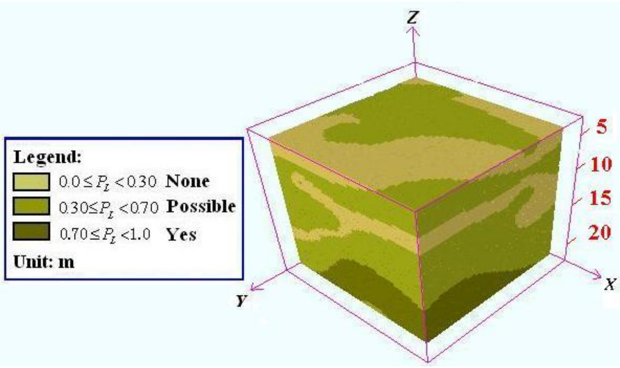

Figure 7 3D liquefaction potential model

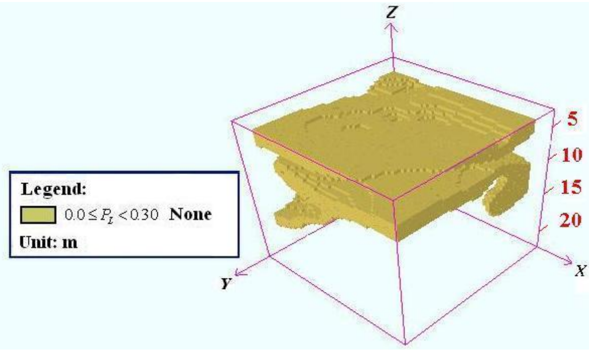

Figure 8 Non-liquefaction soil layers

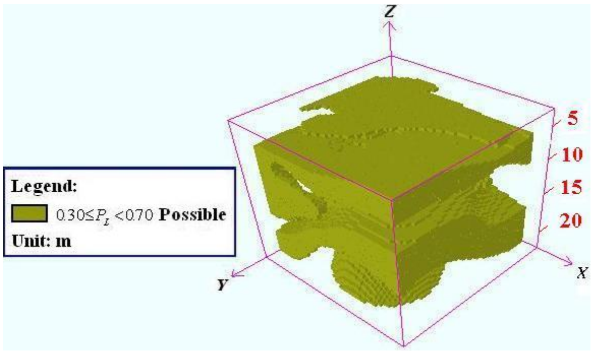

Figure 9 Possible liquefaction soil layers

Figure 11 is the 3D display of the liquefaction potential after body incision. Figure 12 shows the 2D grid cutting profile, which is vertical to x and y axis.

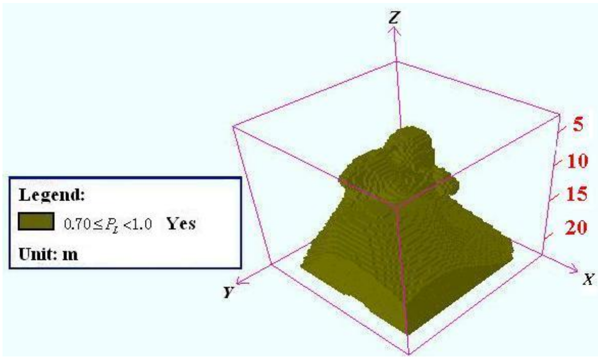

Figure 10 Liquefaction soil layers

As seen from Figure 6 to 12, when the 3D liquefaction potential model is constructed, 2D profile and 3D body incision can be realized and the 3D data filed, which reflect the spatial distributing characteristics of the liquefaction potential, can also be displayed in screen. In practice, when the spatial cutting and incision position is defined, the distributing features of the liquefaction potential in different soil stratums or spatial points can be shown in 2D cutting profile and 3D incision body. Therefore, it will be helpful to researchers to understand the spatial characteristics of the site liquefaction potential from the different visual angle.

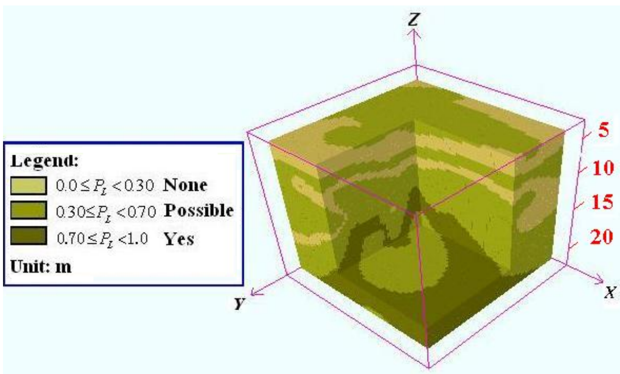

Figure 11 3D liquefaction model after cutting

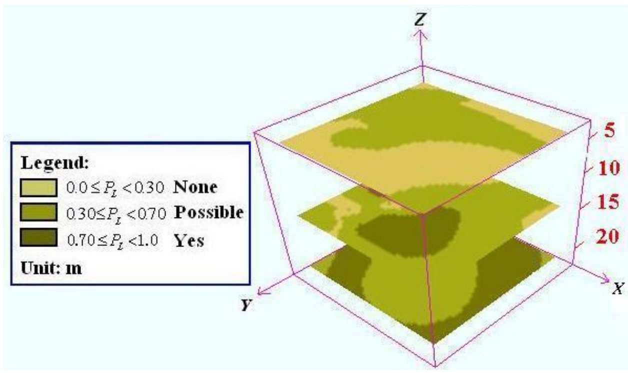

Figure 12 2D GRID display in *XY* and *YZ* plane

4 CONCLUSIONS

(1) When the probability evaluation results are adopted as the "Elevation" in DEM, a "block" data structure is utilized to divide and simulate the 3D liquefaction potential field, and the Kriging interpolation method is utilized to evaluate the liquefaction potential of the unidentified points by the evaluated results of the observation boreholes. The Kriging interpolation is an effect method for evaluating the latent distribution of the site liquefaction potential beyond the observation boreholes. Thus, it is a preferable way to evaluate the possible liquefaction range for a 3D site.

(2) Based on the probability evaluation results and volume rendering technique, Kriging interpolation results are displayed in different color marks to indicate the risk extent of the site liquefaction potential. Thereby, the spatial distributing characteristic and variety trend of the site liquefaction potential can be displayed in a 3D graphic form. Also, the 2D profile cutting and 3D body incision can be generated automatically.

5 ACKNOWLEDGEMENTS

The writers wish to thank the faculty and staff of the Nanjing University of Technology Geotechnical Engineering Institute (GEI) for its support. In particular, wish to thank Professor Chen G. X. for his guidance in earthquake engineering domain. This research is financially supported by the Talent Summit in Six Fields of Jiangsu Province under the grant number 06-F-008 and the PhD Innovation Foundation of NJUT under the grant number BSCX200613.

REFERENCES

O'Rourke T. D. and Pease J.W. (1997). Mapping liquefiable layer thickness for seismic hazard assessment. *Journal of Geotechnical and Geoenvironmental Engineering*, ASCE **123:1**, 46-56.

Zhang L., Shi B. and Wang B. J. (2000). The method to evaluate the sandy soil liquefaction under GIS environment. *Hydrogeology and Engineering Geology* **5:**15-16.

Sun S. L., Gan X. and Zhou Y. D. et al. (2003). Spatial liquefaction analysis of Nanjing subway soil foundationin in view of MapInfo. *Journal of Disaster Prevention and Mitigation Engineering* **23:1**, 80-83.

Tsai K. J., Liaw H. C. and Chu W. P. et al. (2004). Evaluation on soil liquefaction occurred at Taliao Main Depot of Kaohsiung MRT systems in Taiwan. *Chinese Journal of Geotechnical Engineering* **26:3**, 407-411.

Chen, G. X., Li, F. M. (2006). Probabilistic estimation of sand liquefaction based on neural network model of radial basis function. *Chinese Journal of Geotechnical Engineering* **28:3**, 301-305.

Tang, H. (2007). Some key problems in visual evaluation of urban seismic disaster based on GIS. Ph.D Dissertation, Nanjing University of Technology, Nanjing, China.

Chen G. X., Tang H., and Liu J.D. (2008). 3D visualization for earthquake-induced site liquefaction potential based on volume rendering and GIS technology. *Chinese Journal of Geotechnical Engineering* **30:4**, 584-590.

Tang H., Chen G. X., and Liu J.D. (2007). Probabilistic estimation of seismic liquefaction potential for large region site based on two-dimensional GIS technique. *Journal of Disaster Prevention and Mitigation Engineering* **27:3**, 296-301.

Tang, H., Chen, G. X. (2007). Probabilistic estimation of seismic liquefaction potential for 2.5 dimensional site based on GIS. *Journal of Natural Disasters* **16:2**, 86-91.

Xu, H. H, Pan, M. (2005). The application study of volume rendering in the visualization of 3D GIS for geology. *Geography and Geo-Information Science* **21:2**, 6-9.

Li, F. M., Chen G. X., and Cong W. M. (2005). Comprehensive evaluation of sand seismic liquefaction potential in Huai'an city. *Journal of Disaster Prevention and Mitigation Engineering* **25:2**, 216-221.